The minimum of the time-delay wavefront error in Adaptive Optics

Doelman, N.J.

THE MINIMUM OF THE TIME-DELAY WAVEFRONT ERROR IN ADAPTIVE OPTICS

A PREPRINT

Niek Doelman*
Department of Opto-Mechatronics
TNO Industry
Delft, The Netherlands
niek.doelman@tno.nl

June 10, 2019

ABSTRACT

An analytical expression is given for the minimum of the mean square of the time-delay induced wavefront error (also known as the servo-lag error) in Adaptive Optics systems. The analysis is based on the von Kármán model for the spectral density of refractive index fluctuations and the hypothesis of frozen flow. An optimal, temporal predictor can achieve up to a factor 1.77 more reduction of the wavefront phase variance, compared to the – for Adaptive Optics systems commonly used – integrator controller. Alternatively, an optimal predictor can allow for a 1.41 times longer time-delay to arrive at the same residual phase variance as the integrator. In general, the performance of the optimal, temporal predictor depends on the product of time-delay, wind speed and the reciprocal of outer scale.

***K*eywords** Atmospheric Turbulence · Adaptive Optics

1 Introduction

- The residual wavefront error of an astronomical imaging instrument equipped with an Adaptive Optics (AO) system, is determined by several error sources. The instrumental-type errors represent the limitations of the AO system components to cancel the turbulence-induced wavefront distortion. One of the most prominent instrumental AO error sources is the time-delay error, which is due to the overall latency between the sensing and the actual correction of the wavefront. This error is also known as the servo-lag error. In [1] an analytical expression for the time-delay error is given, at a single point, based on the Kolmogorov spectral density and using the integrator as AO controller. The error variance amounts to $28.4(f_G\Delta t)^{5/3}$, with f_G the Greenwood frequency and Δt the time-delay. This expression is often used as a rule-of-thumb in AO performance analysis, design and error budgeting. The integrator controller however does not achieve the minimum possible value of the mean square time-delay error.
The minimum of the mean square time-delay error is obtained by the optimal wavefront phase predictor. In the upcoming sections, the optimal predictor is derived and an analytical expression for the minimum variance of the time-delay error is given. The analysis is based on a stochastic dynamic model for wavefront phase fluctuations. This model follows from a factorization of the von Kármán power spectrum. The stochastic model is the key to finding the optimal predictor of wavefront phase fluctuations over a horizon of the time delay Δt. The properties of optimal prediction are discussed and compared to those of the AO integrator controller.

2 Spectral model

Consider a turbulent atmospheric layer of thickness δh at height h_i and an incident plane wave under a zenith angle ζ. The turbulence is assumed to be stationary, homogeneous and isotropic and is described by the von Kármán model

*2nd affiliation: Leiden Observatory, Leiden University, The Netherlands.

for index-of-refraction fluctuations. The wave distortion after propagation through the thin turbulent layer can be characterised by the covariance function of the wavefront phase fluctuations ([2, 3]) as:

$$C_\phi(r) = \frac{\Gamma(\frac{7}{6})}{\sqrt{2}\,\pi^{\frac{5}{3}}\,\Gamma(\frac{1}{3})} k^2 \delta z C_n^2 {\kappa_0}^{-\frac{5}{3}} (2\pi\kappa_0 r)^{\frac{5}{6}} K_{\frac{5}{6}}(2\pi\kappa_0 r) \tag{1}$$

where $\Gamma(\frac{7}{6})/(\sqrt{2}\,\pi^{\frac{5}{3}}\,\Gamma(\frac{1}{3})) = 0.0363$, $K_{5/6}$ is the modified Bessel function of the second kind of order $5/6$, $\kappa_0 = 1/L_0(h_i)$, $L_0(h_i)$ is the outer scale of the atmospheric turbulent layer, $\delta z = \delta h\,\sec(\zeta)$, k is the wavenumber and $r = |\mathbf{r}|$. The parameter C_n^2 represents the index-of-refraction structure constant at h_i.

The covariance function $C_\phi(r)$ above is circularly symmetric. Taylor's hypothesis of frozen flow implies that for a turbulence variable $u(\mathbf{r}, t)$ it holds, that the future value at $t + \tau$ can be written as a spatially shifted value at t: $u(\mathbf{r}, t + \tau) = u(\mathbf{r} - \mathbf{v}\tau, t)$. Under this hypothesis the spatial covariance function can be converted to a temporal covariance function for a single point by replacing the spatial variable r by $v\tau$; $C_\phi(\tau) = C_\phi(r)$ with $r = v\tau$. Here the variable $v = |\mathbf{v}_\perp|$ represents the modulus of the wind speed perpendicular to the propagation direction at height h_i.

The Fourier Transform of the temporal covariance function, $\int_{-\infty}^{\infty} C_\phi(\tau)\exp(-i\omega\tau)d\tau$, renders the power spectral density (PSD) of phase fluctuations (see eq. 6.699/12 in [4]):

$$\Phi(\omega) = \frac{4}{3}\sqrt{\pi}\,\Gamma(\frac{7}{6})\,k^2\delta z C_n^2 \frac{v^{\frac{5}{3}}}{(\omega^2 + \omega_0^2)^{\frac{4}{3}}} \tag{2}$$

where $\frac{4}{3}\sqrt{\pi}\,\Gamma(\frac{7}{6}) = 2.19$ and $\omega_0 = 2\pi v/L_0$. The frequency ω_0 can be regarded as the angular cut-off frequency in the PSD. The function $\Phi(\omega)$ is double-sided and has unit rad^2/Hz.

The Greenwood frequency $\overline{f_G}$ for the integrated propagation path has been defined as ([5]):

$$\overline{f_G} = \left[\frac{2^{\frac{1}{3}}\,\Gamma(\frac{7}{6})}{3\,\pi^{\frac{7}{6}}} k^2 \int_L C_n^2(z) v^{\frac{5}{3}}(z) dz\right]^{\frac{3}{5}} \tag{3}$$

where $2^{1/3}\,\Gamma(7/6)/3\,\pi^{7/6} = 0.102$ and L is the propagation path. The Greenwood frequency represents the bandwidth of the closed-loop AO system with a first order frequency roll-off (RC-type) that yields a residual phase variance of 1 rad^2 under Kolmogorov turbulence and the given C_n^2 profile. For the case of a single turbulent layer at h_i the Greenwood frequency f_G can be expressed as:

$$f_G = \left[\frac{2^{\frac{1}{3}}\,\Gamma(\frac{7}{6})}{3\,\pi^{\frac{7}{6}}}\,k^2 C_n^2(h_i) v^{\frac{5}{3}}(h_i)\delta z\right]^{\frac{3}{5}} \tag{4}$$

Inserting f_G into the expression for the PSD (2) gives

$$\Phi(\omega) = \frac{(2\pi f_G)^{\frac{5}{3}}}{(\omega^2 + \omega_0^2)^{\frac{4}{3}}} \tag{5}$$

In the limit of an unbounded outer scale $L_0 \to \infty$ and therefore $\omega_0 \downarrow 0$, the expression for the power spectral density is reduced to

$$\Phi_{Kol}(\omega) = (2\pi f_G)^{\frac{5}{3}} \omega^{-\frac{8}{3}} \tag{6}$$

This is in fact the power spectral density for the case of Kolmogorov turbulence and is in full agreement with eq.(11) in [1].

The variance of the uncorrected or primary wavefront phase fluctuations - $C_\phi(r)$ for $r = 0$ in (1) - amounts to:

$$\sigma^2_{prim} = \frac{3\,\Gamma(\frac{5}{6})}{2\sqrt{\pi}\Gamma(\frac{1}{3})}\left(\frac{f_G}{f_0}\right)^{\frac{5}{3}} \tag{7}$$

where $3\Gamma(\frac{5}{6})/(2\sqrt{\pi}\Gamma(\frac{1}{3})) = 0.357$ and $f_0 = \omega_0/(2\pi) = v/L_0$. The primary variance increases with the $5/3$ power of the f_G/f_0 fraction. For Kolmogorov turbulence the variance is unbounded.

3 Stochastic process model

3.1 Spectral factor

Modeling the wavefront phase fluctuations $\phi(t)$ as a real, wide-sense stationary random process, $\phi(t)$ can be represented in an innovations model form:

$$\phi(t) = \int_0^\infty h(\tau)\xi(t-\tau)d\tau \tag{8}$$

where ξ is zero-mean white noise process, with auto-covariance function: $R_{\xi\xi}(\tau) = \delta(\tau)$. The causal innovations filter $h(\tau)$ is the impulse response of transfer function $H(s)$, which is the minimum-phase spectral factor of the power spectrum $\Phi(s)$, such that $\Phi(s) = H(s)H(-s)$, see [6]. By taking the Laplace transform of the covariance function (1), $\int_{-\infty}^{\infty} C_\phi(\tau)\exp(-s\tau)d\tau$, the power spectrum $\Phi(s)$ is obtained as

$$\Phi(s) = \frac{(2\pi f_G)^{\frac{5}{3}}}{(-s^2+\omega_0^2)^{\frac{4}{3}}} \tag{9}$$

This power spectrum (9) obeys the Paley-Wiener criterion. Its minimum-phase spectral factor can be readily found by taking the left-hand side roots of $\Phi(s)$:

$$H(s) = \frac{(2\pi f_G)^{\frac{5}{6}}}{(s+\omega_0)^{\frac{4}{3}}} \tag{10}$$

The impulse response of the spectral factor (10) follows by taking the inverse Fourier transform:

$$h(\tau) = \frac{1}{2\pi}\int_{-\infty}^{\infty} H(i\omega)\exp(i\omega\tau)d\omega = \frac{(2\pi f_G)^{\frac{5}{6}}}{\Gamma(\frac{4}{3})}\,\tau^{\frac{1}{3}}\exp(-\omega_0\tau) \tag{11}$$

see eq. 3.382/6 in [4]). The impulse response (11) is causal, $h(\tau) = 0$ for $\tau < 0$.

3.2 Related model families

The covariance function of wavefront phase fluctuations (1) belongs to the family of Matérn functions ([7]). In the particular case of the von Kármán model, the Matérn smoothness parameter equals $5/6$.

In the discrete time domain, the tempered fractionally integrated ARMA model, denoted as ARTFIMA model ([8]), can be seen as a stochastic process model for von Kármán type phase fluctuations. In accordance with (1), the ARTFIMA fractional integration parameter then equals $4/3$ and the tempering parameter is determined by ω_0. The ARTFIMA model could be suitable for simulation purposes of wavefront phase fluctuations.

4 The minimum prediction error

To determine the minimum of the mean square time-delay error, the optimal prediction of the phase fluctuations $\phi(t)$ needs to be formulated. Given the overall time-delay Δt of the AO loop, at time instant t the future value $\phi(t+\Delta t)$ is to be predicted based on its time history $\phi(t-\tau)$, with $\Delta t > 0$ and $\tau \geq 0$. Note that the predictor relies on temporal information only. Denoting the predictor as a causal linear, time-invariant (LTI) filter P, the prediction of $\phi(t+\Delta t)$ can be expressed as:

$$\widehat{\phi}(t+\Delta t) = \int_0^\infty p(\tau)\phi(t-\tau)d\tau \tag{12}$$

Based on the innovations model (8, 11), the optimal prediction filter of $\phi(t)$ over an horizon Δt can be derived, see [6]. The Laplace domain optimal predictor equals:

$$P_{opt}(s) = \frac{1}{H(s)}\int_0^\infty h(\tau+\Delta t)\exp(-s\tau)d\tau \tag{13}$$

Inserting the spectral factor (10) and (11) yields:

$$P_{opt}(s) = \frac{1}{\Gamma(\frac{4}{3})}\exp(s\Delta t)\Gamma_u(\frac{4}{3},(s+\omega_0)\Delta t) \tag{14}$$

where Γ_u is the upper incomplete gamma function: $\Gamma_u(a,x) = \int_x^\infty t^{a-1}\exp(-t)dt$. The corresponding minimum of the mean square time-delay error can be written as ([6]):

$$\sigma^2_{min} = \int_0^{\Delta t} h^2(\tau)d\tau \tag{15}$$

Using (11), this minimum mean square error equals:

$$\sigma^2_{min} = \frac{1}{\Gamma^2(\frac{4}{3})}\left(\frac{f_G}{2f_0}\right)^{\frac{5}{3}}\gamma_\ell(\frac{5}{3}, 2\omega_0\Delta t) \tag{16}$$

where γ_ℓ is the lower incomplete gamma function: $\gamma_\ell(a,x) = \int_0^x t^{a-1}\exp(-t)dt$.

5 Prediction error with integrator control

The essence of the common control approach in AO systems is to feed the latest (measured) wavefront phase value, with opposite sign, back to the optical wavefield. Equivalently, in a closed-loop control setting the latest residual wavefront phase value is added – with opposite sign – to the previous phase correction. From a control perspective this approach can be characterised as an integrator control law. In [9] this strategy is also denoted as zero-order prediction. To evaluate the prediction performance of the integrator, the open-loop control setting is considered here. In the form of the prediction expression (12), the transfer function of the effective predictor with integrator control is $P_{int}(s) = 1$. Given the AO system delay Δt, this leads to the following residual error:

$$\epsilon_{int}(t) = \phi(t+\Delta t) - \phi(t) \tag{17}$$

Following [1] the mean square of this error could be evaluated in the Fourier domain. Alternatively, the von Kármán structure function $D_\phi(r)$ of wavefront phase fluctuations can be evaluated for $r = v\Delta t$, as D_ϕ exactly represents the variance of differenced wavefront phase fluctuations. Using the relation between the structure function and the covariance function (1), the residual error variance for the integrator approach is obtained as:

$$\begin{aligned}\sigma^2_{int} &= D_\phi(v\Delta t) = 2\left[\sigma^2_\phi - C_\phi(v\Delta t)\right] \\ &= \frac{1}{\sqrt{\pi}\,\Gamma(\frac{4}{3})}\left(\frac{f_G}{f_0}\right)^{\frac{5}{3}}\left[\Gamma(\frac{5}{6}) - 2^{\frac{1}{6}}(\omega_0\Delta t)^{\frac{5}{6}}K_{\frac{5}{6}}(\omega_0\Delta t)\right]\end{aligned} \tag{18}$$

where $K_{5/6}$ is the modified Bessel function of the second kind of order $5/6$.

Note that with the open-loop perspective on the prediction performance, the closed-loop stability properties of this control approach have not been taken into account.

6 Case of Kolmogorov Turbulence

The expressions for residual phase error variance (16) and (18) hold for any non-negative value of the time-delay Δt. In practice, the delay will be limited and the product $\omega_0\Delta t$ will be much smaller than unity, even for a high wind speed and a small outer scale. Evaluation of a series expansion of (16) and (18) for small $\omega_0\Delta t$ leads to:

$$\sigma^2_{min} \approx (2\pi f_G\Delta t)^{5/3}\left[0.753 - 0.941(\omega_0\Delta t) + \mathcal{O}(\omega_0\Delta t)^2\right] \tag{19}$$

$$\sigma^2_{int} \approx (2\pi f_G\Delta t)^{5/3}\left[1.33 - 1.07(\omega_0\Delta t)^{\frac{1}{3}} + \mathcal{O}(\omega_0\Delta t)^2\right] \tag{20}$$

For the specific case of Kolmogorov turbulence, in the limit of $L_0 \to \infty$ and so $f_0 \downarrow 0$, the expressions for the residual variances reduce to:

$$\lim_{f_0\downarrow 0}\sigma^2_{min} = \frac{3}{5\,\Gamma^2(\frac{4}{3})}(2\pi f_G\Delta t)^{\frac{5}{3}} \approx 16.1(f_G\Delta t)^{\frac{5}{3}} \tag{21}$$

$$\lim_{f_0\downarrow 0}\sigma^2_{int} = \frac{3}{5}\frac{\Gamma(\frac{1}{6})}{2^{\frac{2}{3}}\sqrt{\pi}\Gamma(\frac{4}{3})}(2\pi f_G\Delta t)^{\frac{5}{3}} \approx 28.4(f_G\Delta t)^{\frac{5}{3}} \tag{22}$$

Note that the expression for σ^2_{int} is equal to eq. (20) in [1].
Both residual variances increase with the $5/3$ power of the product $f_G\Delta t$. The minimum wavefront phase error with the optimal predictor is a factor $[\Gamma(\frac{4}{3})\Gamma(\frac{1}{6})]/[2^{\frac{2}{3}}\sqrt{\pi}] = 1.77$ smaller than with the integrator approach.

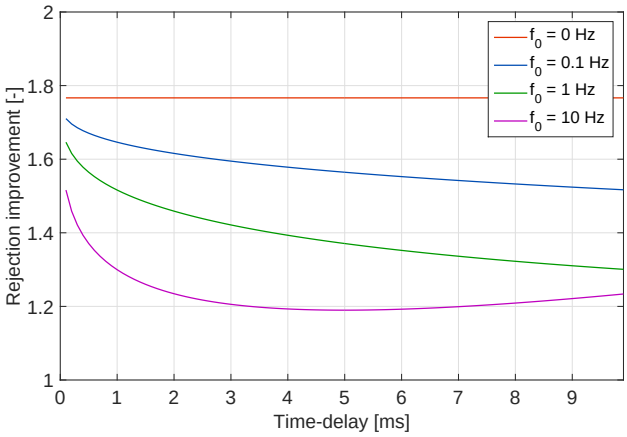

Figure 1: Improvement on variance reduction of predictor versus integrator ($\sigma^2_{int}/\sigma^2_{min}$) for small time-delays and various values of f_0.

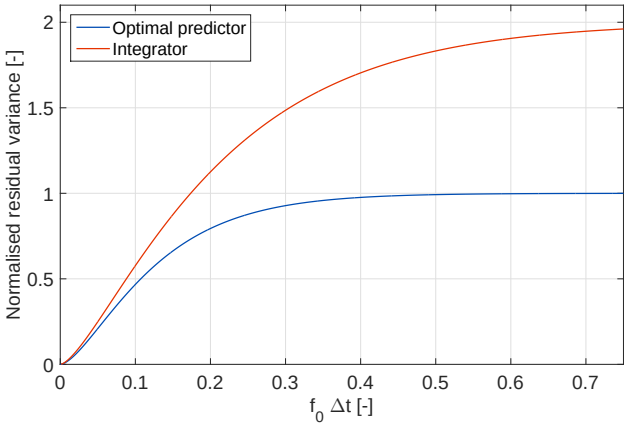

Figure 2: Normalised residual phase variances $\sigma^2_{min}/\sigma^2_{prim}$ and $\sigma^2_{int}/\sigma^2_{prim}$ against $f_0\Delta t$.

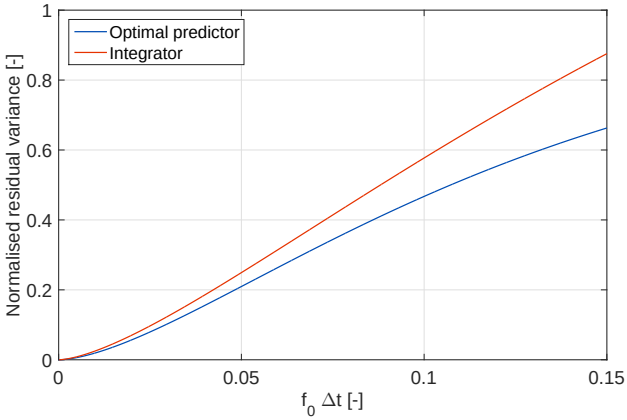

Figure 3: Normalised residual phase variances $\sigma^2_{min}/\sigma^2_{prim}$ and $\sigma^2_{int}/\sigma^2_{prim}$ against small values of $f_0\Delta t$.

7 Analysis

The optimal predictor (14) is a function of time-delay Δt, wind speed v and outer scale L_0. It does not depend on for instance the wavenumber k, zenith angle ζ or the index-of-refraction structure constant C_n^2.

From (7), (16) and (18) it follows that the minimum of the mean square time-delay error increases with Δt and decreases with f_0. Similar to the primary variance and the residual phase variance with the integrator, the minimum variance grows with the $5/3$ power of the Greenwood frequency. In addition, the normalised residual variance ($\sigma^2_{res}/\sigma^2_{prim}$) is a function of the product $f_0\Delta t$, for both the optimal predictor and the integrator.

The optimal predictor always performs better than the integrator; see Figures 1, 2 and 3. For small values of $f_0\Delta t$, the improvement on phase variance reduction ranges from a factor 1.19 (for $f_0\Delta t = 0.05$) up to 1.77 for $f_0\Delta t = 0$, which represents the Kolmogorov turbulence case. For large $f_0\Delta t$, the optimal predictor becomes ineffective and achieves no phase error reduction (for $f_0\Delta t > 0.4$) . For the integrator, a large $f_0\Delta t$ value (> 0.75) leads to doubling of the primary variance, as phase disturbance values large Δt apart are fully uncorrelated; see Figure 2. Note, that these large $f_0\Delta t$ values are unlikely in practical cases.

Apart from a smaller temporal wavefront error, another benefit of optimal prediction in AO systems would be to allow for a longer detector integration time and therefore the use of a fainter reference star. Equalising the expressions for the residual variance, (21) and (22) for the Kolmogorov case, gives the following relation between the delay times:

$$\Delta t_{opt} = \left[\frac{\Gamma(\frac{4}{3})\Gamma(\frac{1}{6})}{2^{\frac{2}{3}}\sqrt{\pi}}\right]^{\frac{3}{5}} \Delta t_{int} \approx 1.41\Delta t_{int} \tag{23}$$

So the detector integration time with an optimal predictor can be 1.41 times longer compared to the integrator case. This would allow a higher reference star magnitude and would improve the sky coverage.

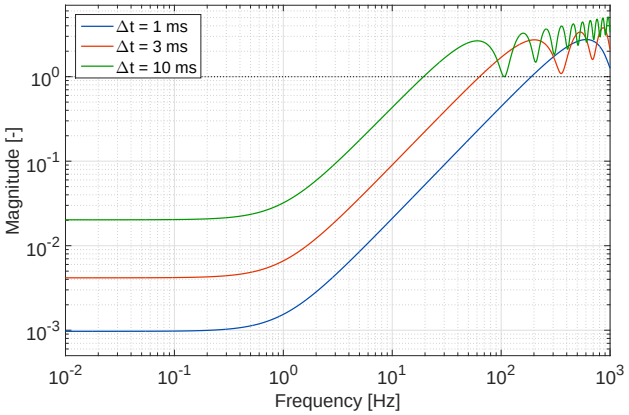

Figure 4: Optimal predictor sensitivity function for f_0 = 1 Hz and various values of Δt.

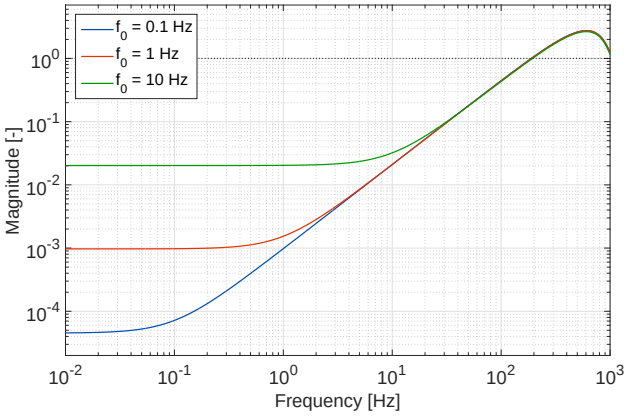

Figure 5: Optimal predictor sensitivity function for Δt = 1 ms and various values of f_0.

The spectral behaviour of optimal prediction is shown in Figures 4 and 5, which reveal the modulus of the transfer function from input phase error to residual error (i.e. the sensitivity function). Figure 4 shows that the bandwidth of rejection reduces with the time-delay. The sensitivity curve crosses the unity magnitude line at approximately $(1/5\Delta t)$ Hz. For a fixed time-delay, the bandwidth of rejection is independent of the cut-off frequency f_0. Only the

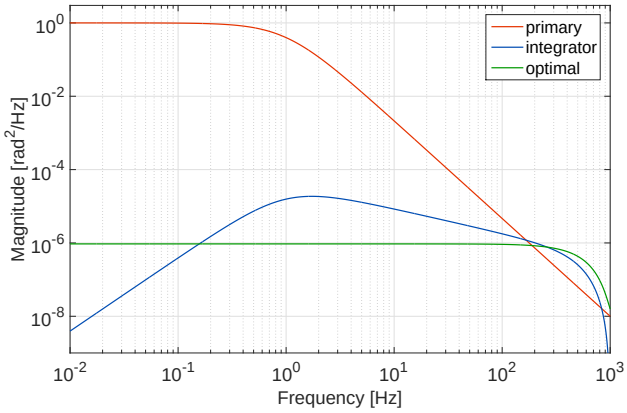

Figure 6: Power Spectral Density of phase fluctuations for the uncorrected case, the integrator and the optimal predictor for Δt = 1 ms and f_0 = 1 Hz.

degree of low-frequency attenuation is affected by f_0; see Figure 5. In terms of the PSD of residual phase fluctuations the optimal predictor achieves a flat spectrum over a large frequency band. It outperforms the integrator in the mid-frequency range, whereas the integrator obtains a higher low-frequency rejection; see Figure 6. Both approaches have about the same frequency bandwidth of rejection and give rise to an increase of the high-frequency phase error.

8 Path-integrated turbulence

So far the analysis of residual wavefront errors has been restricted to propagation through a single, thin layer of turbulence. The atmosphere for the overall propagation path can be viewed as built up from multiple turbulent layers at different heights. For a plane wave and under the geometrical optics approximation, the path-integrated power spectrum of wavefront phase fluctuations $\overline{\Phi}(\omega)$ can then be written as ([2]):

$$\overline{\Phi}(\omega) = \frac{4}{3}\sqrt{\pi}\,\Gamma(\frac{7}{6})\,k^2 \int_L dz\, C_n^2(z) \frac{v^{\frac{5}{3}}(z)}{(\omega^2 + \omega_0^2(z))^{\frac{4}{3}}} \tag{24}$$

Here, the PSD cut-off frequency ω_0 is a function of height, since both the outer scale L_0 and the wind vector $\mathbf{v}$ are height-dependent. In fact, each turbulent layer has its own, specific PSD cut-off frequency. This prevents getting a similar compact form for the overall power spectrum as in (2) for a single layer. Following the approach proposed by several authors ([3, 2, 10]), an effective cut-off frequency $\overline{\omega_0}$ could be used instead. The $\overline{\omega_0}$ value is then set such as to minimise the discrepancy between the true and approximated power spectrum for instance. This metric can be quantified as:

$$\epsilon(\omega_c) = \int_{-\infty}^{\infty} d\omega \left[\overline{\Phi}(\omega, \omega_c) \;\; - \;\; \overline{\Phi}(\omega)\right]^2 \tag{25}$$

where $\overline{\Phi}(\omega, \omega_c)$ is $\overline{\Phi}(\omega)$ of eq. (24) with $\omega_0(z)$ replaced by the constant ω_c. The optimal value of ω_c for which $\epsilon(\omega_c)$ is minimised is denoted as $\overline{\omega_0}$. With the optimal value of the effective cut-off frequency in place, the path-integrated wavefront phase (24) PSD becomes:

$$\overline{\Phi}(\omega) = \frac{(2\pi\overline{f_G})^{\frac{5}{3}}}{\left(\omega^2 + \overline{\omega_0}^2\right)^{\frac{4}{3}}} \tag{26}$$

This power spectrum has exactly the same form as for the single layer case (5). And therefore, the full performance analysis of optimal and integrator prediction (section 7) also holds for the approximated path-integrated case with multiple turbulent layers. Note that for Kolmogorov turbulence specifically, the results section 7 are still exact as then the cut-off frequency ω_0 plays no role.

9 Conclusion

Analytical expressions for the minimum time-delay induced wavefront phase error and the optimal predictor have been presented. The specific performance and spectral properties have been analysed. In comparison to the integrator, the

performance gain of optimal prediction can be significant. In more detail, the gain depends on the product of time-delay, wind speed and the reciprocal of outer scale $v\Delta t/L_0$. The largest performance advantage is obtained for small values of $v\Delta t/L_0$ ($< 10^{-3}$). For larger values – up to $v\Delta t/L_0 = 0.2$ – the performance gain is modest.

The analysis has been focused on wavefront phase prediction in an open-loop setting. Closed-loop aspects have not been taken into account. On the other hand, further reduction of the time-delay error could be achieved when accounting for the spatial properties of frozen flow. If Taylor's hypothesis of frozen flow is valid, then wind-upstream sensor nodes would contain information of the future wavefront phase at wind-downstream sensor nodes. This enables the use of a feedforward-type prediction filter structure, leading to a higher reduction of the time-delay error (except for the sensor nodes at the upstream edge).

References

[1] David L Fried. Time-delay-induced mean-square error in adaptive optics. *JOSA A*, 7(7):1224–1225, 1990.

[2] Larry C Andrews and Ronald L Phillips. *Laser beam propagation through random media*, volume 152. SPIE press Bellingham, WA, 2005.

[3] Rodolphe Conan. Mean-square residual error of a wavefront after propagation through atmospheric turbulence and after correction with zernike polynomials. *JOSA A*, 25(2):526–536, 2008.

[4] Izrail Solomonovich Gradshteyn and Iosif Moiseevich Ryzhik. *Table of integrals, series, and products*. Academic press, 2007.

[5] Darryl P Greenwood. Bandwidth specification for adaptive optics systems. *JOSA*, 67(3):390–393, 1977.

[6] Athanasios Papoulis and S Unnikrishna Pillai. Probability, random variables, and stochastic processes. *Mc-Graw Hill*, 1991.

[7] Bertil Matérn. *Spatial Variation: Stochastic Models and Their Application to Some Problems in Forest Surveys and Other Sampling Investigations*. Statens skogsforskningsinstitut, 1960.

[8] Mark M Meerschaert, Farzad Sabzikar, Mantha S Phanikumar, and Aklilu Zeleke. Tempered fractional time series model for turbulence in geophysical flows. *Journal of Statistical Mechanics: Theory and Experiment*, 2014(9):P09023, 2014.

[9] John W Hardy. *Adaptive optics for astronomical telescopes*, volume 16. Oxford University Press, 1998.

[10] VP Lukin, EV Nosov, and BV Fortes. The efficient outer scale of atmospheric turbulence. In *European Southern Observatory Conference and Workshop Proceedings*, volume 56, page 619, 1999.